Surface Tension, Pressure Difference and Laplace Formula for Membranes

Hiroshi Koibuchi

Department of Mechanical and Systems Engineering, National Institute of Technology, Ibaraki College, Nakane 866, Hitachinaka, Ibaraki 312-8508, Japan

E-mail: koibuchi@mech.ibaraki-ct.ac.jp

Andrey Shobukhov

Faculty of Computational Mathematics and Cybernetics, Lomonosov Moscow State University, 119991, Moscow, Leninskiye Gory, MSU, 2-nd Educational Building, Russia

The surface tension γ and the pressure difference Δp for spherical membranes are calculated using Monte Carlo simulation technique. We study the so-called tethered and fluid surface discrete models that are defined on the fixed-connectivity (tethered) and dynamically triangulated (fluid) lattices respectively. Hamiltonians of the models include a self-avoiding potential, which makes the enclosed volume well defined. We find that there is reasonable accuracy in the technique for the calculation of γ using the real area A if the bending rigidity κ or A/N is sufficiently large. We also find that γ becomes constant in the limit of $A/N \to \infty$ both in the tethered and fluid surfaces. The property $\lim_{A/N\to\infty}\gamma = \text{const}$ corresponds to certain experimental results in cell biology.

Keywords: Membranes, Triangulated surfaces, Surface tension, Laplace pressure, Monte Carlo

1. Introduction

The surface tension γ [1, 2, 3] and the pressure difference $\Delta p = p_{\rm in} - p_{\rm out}$, where $p_{\rm in}(p_{\rm out})$ is the pressure inside (outside) the surface, potentially reflect the microscopic interactions of the constituent molecules. Therefore, it is interesting to study γ and Δp by means of stochastic simulation of mechanical processes on the triangulated surface models such as Helfrich-Polyakov (HP) [4, 5]. The HP model is a coarse grained mathematical model for the microscopic interactions of lipid molecules [6]. The frame tension τ is defined via the macroscopic surface energy, which equals τA_p, where A_p is the projected area. This A_p may be regarded as the area contained within the boundary $\Gamma(\subset \mathbf{R}^2)$ fixed in $\mathbf{R}^3$ [7, 8]. For this reason, it is widely accepted that on the surfaces spanning Γ the frame tension τ is correctly calculated by using the projected area A_p of Γ rather than the real area A of the surface.

However, A_p is not always well-defined on the surfaces without boundary. In fact, we can use only the real area A in both simulations and data analyses. Therefore we have the surface tension γ of the HP model defined on spherical surface which has no boundary and the frame tension τ evaluated by Δp and the Laplace formula. Thus, we should prove that γ may be

correctly defined through the real area A by comparing it with τ. γ and τ are expected to be identical in the limit of $\kappa(\sim 1/k_BT) \to \infty$ [8].

In this paper, we calculate the surface tension γ for spherical membranes and check whether γ is consistent with the frame tension τ, which is obtained from Δp and the Laplace formula.

2. Model

The partition function Z is defined by

$$Z = \sum_{\mathcal{T}} \int' \prod_{i=1}^{N} d\mathbf{r}_i \exp\left[-S(\mathbf{r}, \mathcal{T})\right], \tag{1}$$

where $\sum_{\mathcal{T}}$ denotes the sum over all possible triangulations $\mathcal{T}$. This $\sum_{\mathcal{T}}$ is included in Z only for the fluid surface model; the fixed-connectivity model is defined by Z without $\sum_{\mathcal{T}}$. The prime in $\int' \prod_{i=1}^{N} d\mathbf{r}_i$ denotes that the center of mass of the surface is fixed to the origin of $\mathbf{R}^3$, and the surface has no boundary Γ. The discrete Hamiltonian $S(\mathbf{r}, \mathcal{T})$ is defined on a triangulated sphere with $\mathbf{r}_i (i=1, \cdots, N)$, which are the positions of vertices, and $\mathcal{T}$ such that

$$\begin{aligned} &S(\mathbf{r}, \mathcal{T}; \kappa, A_0, \Delta p) = S_1 + \kappa S_2 + U_{\mathrm{Fix}}(A_0) - \Delta p V + U_{\mathrm{S}}, \\ &S_1 = \sum_{ij} (\mathbf{r}_i - \mathbf{r}_j)^2, \quad S_2 = \sum_{ij} (1 - \mathbf{n}_i \cdot \mathbf{n}_j), \end{aligned} \tag{2}$$

where S_1 is the Gaussian bond potential and S_2 the bending energy with the bending rigidity $\kappa[1/k_BT]$. The symbol $\mathbf{n}_i$ denotes the unit normal vector of the triangle i, and $\sum_{ij}$ of S_1 and S_2 denote the sum over all nearest neighbor vertices and triangles respectively. The potential $U_{\mathrm{Fix}}(A_0)$, which fixes the surface area A to a constant A_0 without using the boundary Γ, is defined by

$$U_{\mathrm{Fix}}(A_0) = \begin{cases} \infty & (|1 - A/A_0| > \epsilon_A = 1/N_T), \\ 0 & (\text{otherwise}), \end{cases} \tag{3}$$

where N_T is the total number of triangles $N_T = 2N-4$. Note that the surface is allowed to have only in-plane deformation if ϵ_A is exactly zero, therefore ϵ_A should be fixed to a small positive number. The energy $-\Delta p V$ with the enclosed volume V is well-defined only for the self-avoiding (SA) surface models [9]. Thus, the energy $-\Delta p V$ must be included in the Hamiltonian together with the SA potential U_{S} defined by $U_{\mathrm{S}} = \sum_{\Delta\Delta'} U_{\mathrm{S}}(\Delta, \Delta')$ where $\sum_{\Delta\Delta'}$ denotes the sum over all non-nearest neighbor triangles and

$$U_{\mathrm{S}}(\Delta, \Delta') = \begin{cases} \infty & (\text{triangles } \Delta\Delta' \text{ intersect}), \\ 0 & (\text{otherwise}). \end{cases} \tag{4}$$

This potential is considered as an extension of the one of Doi-Edwards model for polymers [10].

The partition function Z is independent of the change in the integration variables $\mathbf{r} \to \mathbf{r}'$. This property is called the scale invariance, which can be expressed by $\partial_\alpha \log Z(\alpha \mathbf{r})|_{\alpha=1} = 0$. The surface tension γ is obtained from this property as follows: It is easy to see that S_2 and U_{S} are scale independent and that $S_1(\alpha \mathbf{r}) = \alpha^2 S_1(\mathbf{r})$, $\Delta p V(\alpha \mathbf{r}) = \alpha^3 \Delta p V(\mathbf{r})$. Since $U_{\mathrm{Fix}}(A_0; \alpha \mathbf{r}) = U_{\mathrm{Fix}}(\alpha^{-2} A_0; \mathbf{r})$, we see that the corresponding derivative $\partial_\alpha \log Z(A_0; \alpha \mathbf{r})|_{\alpha=1}$ can be written as $-2A_0 \partial_{A_0} \log Z(A_0; \mathbf{r})$. Note that the partition function for the macroscopic membranes is given by

$$Z_{\mathrm{mac}} = \exp\left[-(\gamma A - \Delta p V)\right], \tag{5}$$

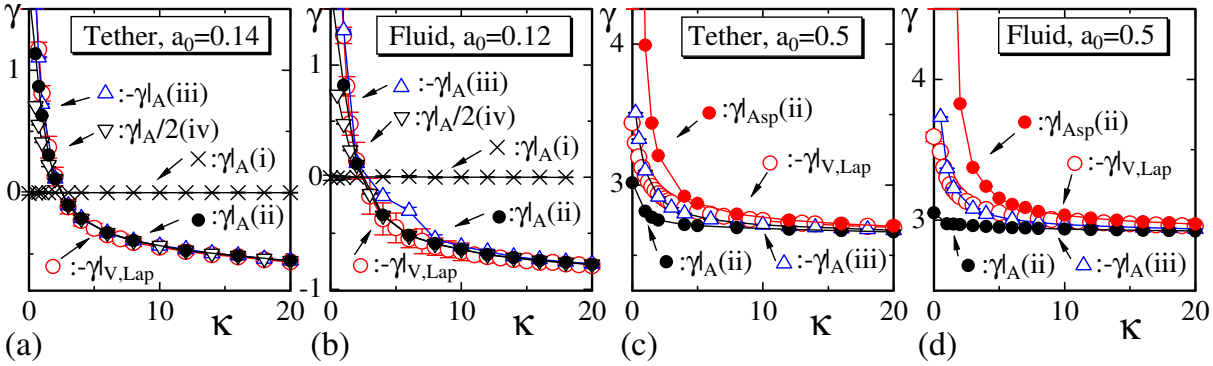

Figure 1. γ vs. κ at (a) $a_0(=A_0/N_T)=0.14$ (tethered), (b) $a_0=0.12$ (fluid), (c) $a_0=0.5$ (tethered) and (d) $a_0=0.5$ (fluid). The symbols ◯ ($\times$, ●, △, ▽) denote the results obtained by the constant volume (area) simulations. The lattice size is $N=1442$.

where V is the enclosed volume. We have

$$\gamma|_A = (2\langle S_1\rangle_{A,\Delta p} - 3\Delta p\langle V\rangle_{A,\Delta p} - 3N)/(2A_0), \tag{6}$$

where $\langle S_1\rangle_{A,\Delta p}$ and $\langle V\rangle_{A,\Delta p}$ are obtained by the constant area simulations.

The pressure difference Δp in $Z_{\rm mac}$ of Eq. (5) can also be calculated using almost the same model and procedure as those described above for $\gamma|_A$. Indeed, the constraint $U_{\rm Fix}(A_0)$ in Eq. (2) can be replaced by $U_{\rm Fix}(V_0)$ to fix the enclosed volume V to V_0; and the energy $-\Delta pV$ should be removed from the Hamiltonian. In this model, Δp is not an input parameter but an output. Thus, the Hamiltonian is given by replacing A_0 with V_0 in Eq. (3) such that $S(\mathbf{r},\mathcal{T};\kappa,V_0)=S_1+\kappa S_2+U_{\rm Fix}(V_0)+U_{\rm S}$.

From the scale invariance of Z in Eq. (1) and $Z_{\rm mac}$ in Eq. (5), we obtain

$$\Delta p|_V = (3N - 2\langle S_1\rangle_V)/(3V_0). \tag{7}$$

The symbol $\Delta p|_V$ is used for the calculated pressure to distinguish it from the input parameter Δp in Eq. (2). It must be emphasized that $\Delta p|_V$ does not suffer from the problem encountered in the calculation of $\gamma|_{A_p}$.

3. Simulation results

The variables $\mathbf{r}$ and $\mathcal{T}$ are updated by the canonical Metropolis MC technique, where $\mathcal{T}$ is updated by using the standard bond flip technique. We use the surface of size $N=1442$. The total number of MCS is about 5×10^6 including 5×10^5 thermalization MCS.

3.1. Dependence of $\gamma|_A$ on κ

We firstly perform MC simulations by varying κ with constant V_0 to check whether the MC results of $\gamma|_A$ are consistent with those of $\Delta p|_V$. The constant V_0 is fixed by the triangle areas so that the mean value $a_0=A_0/N_T$ becomes $a_0=0.14$ (tethered model) and $a_0=0.12$ (fluid model). From the MC results $\Delta p|_V$ of the tethered and fluid models we obtain $\gamma|_{V,\rm Lap}$ using the Laplace formula

$$\gamma|_{V,\rm Lap} = (2/R)\Delta p|_V, \quad R=(3V_0/4\pi)^{1/3}. \tag{8}$$

These results are plotted (◯) in Figs. 1(a)–(d). This $\gamma|_{V,\rm Lap}$ is completely different from $\gamma|_A$ because $\gamma|_{V,\rm Lap}$ ($\gamma|_A$) is obtained by the constant volume (area) simulations. Indeed, the sign

of $\gamma(=\gamma|_A)$ of the surface expanded by its area in general is different from $\gamma(=\gamma|_{V,\mathrm{Lap}})$ of the same surface expanded by its volume. This comes from the definition of Z_{mac} in Eq. (5). Note also that the surface shape remains spherical in the constant V_0 simulations even in the limit of $\kappa\to 0$ for both tethered and fluid models.

Next, we perform the simulations with constant area A_0 and Δp such that $A_0=\langle A\rangle_V$ and

$$\text{(i)}\Delta p=-\Delta p|_V,\quad \text{(ii)}\Delta p=0,\quad \text{(iii)}\Delta p=-2\Delta p|_V,\quad \text{(iv)}\Delta p=\Delta p|_V, \tag{9}$$

where $\langle A\rangle_V$ and $\Delta p|_V$ are the output of the first simulations. Under these four different conditions, we obtain the surface tensions $\gamma|_A$ from Eq. (6). We predict that the simulation results $\gamma|_A(\kappa)$ satisfy

$$\text{(i)}\gamma|_A=0(\times),\quad \text{(ii)}\gamma|_A=-\gamma|_{V,\mathrm{Lap}}(\bullet),\quad \text{(iii)}\gamma|_A=\gamma|_{V,\mathrm{Lap}}(\triangle),\quad \text{(iv)}\gamma|_A=-2\gamma|_{V,\mathrm{Lap}}(\triangledown). \tag{10}$$

These equalities correspond to the conditions in Eq. (9) (see Fig. 1).

The predictions in Eq. (10) come from the expectations

$$V_0=\langle V\rangle_{A,\Delta p},\quad \langle S_1\rangle_V=\langle S_1\rangle_{A,\Delta p}, \tag{11}$$

which are independent of Δp. It is easy to prove the predictions in Eq. (10) using Eq. (11). These equations are physically almost clear because the enclosed volume V_0 is uniquely determined by its surface area A_0 if the surface is a sphere. Figure 1 (b) shows that (iii) $\gamma|_A=\gamma|_{V,\mathrm{Lap}}$ is slightly broken in the region $\kappa\simeq 5$. The reason of this deviation is that the surface shape becomes prolate under the negative pressure $\Delta p=-2\Delta p|_V$ at $\kappa\simeq 5$ [11, 12].

The prediction (ii) of Eq. (10) in the small κ region is broken as we see in Figs. 1(c),(d). This deviation appears only because of the difference between A_0 and A_p expected in that region. Indeed, $\gamma|_{\mathrm{A}}$ ($\gamma|_{\mathrm{A_{sp}}}$) is slightly smaller (larger) than $-\gamma|_{V,\mathrm{Lap}}$, where $\gamma|_{\mathrm{A_{sp}}}$ is calculated by replacing A_0 with $A_{\mathrm{sp}}=4\pi\left(3\langle V\rangle_A/4\pi\right)^{2/3}$ in Eq. (6). This discrepancy implies that A_p is in the range $A_{\mathrm{sp}}<A_p<A_0$, because $\gamma|_{V,\mathrm{Lap}}$ in Eq. (8) is expected to be correct due to the fact that the surface remains spherical in the volume constant simulation in the whole region of κ as mentioned above. Note that the prediction (i) of Eq. (10), which is not depicted, is satisfied also in the whole region of κ including $\kappa=0$ for $a_0=0.5$.

3.2. Dependence of γ on A/N

Now we proceed to an additional check for the MC results of $\gamma|_A$ and $\gamma|_{V,\mathrm{Lap}}$ obtained by the area and volume constant simulations, respectively, by varying $A_0/N_T(=a_0)$ with fixed κ. In contrast to the check described above, these two different simulations can be performed independently. Thus we obtain $\Delta p|_V$, from which $\gamma|_{V,\mathrm{Lap}}$ is calculated by using the Laplace formula in Eq. (8). Therefore we expect that the simulation results satisfy (see Figs. 2(a)–(h))

$$-\gamma|_{V,\mathrm{Lap}}(\bullet)=\bar{\gamma}|_{A,\Delta p}(\bigcirc),\quad \text{with}\quad \bar{\gamma}|_{A,\Delta p}:=\left(2\langle S_1\rangle_{A,\Delta p}-3N\right)/(2A_0). \tag{12}$$

The expectation in Eq. (12) is obtained by using the relations (as functions of a_0)

$$A_0=\langle A\rangle_V,\quad \langle S_1\rangle_{A,\Delta p}=\langle S_1\rangle_V. \tag{13}$$

These relations also explain why we expect the surface areas to be the same in both simulations at least for sufficiently large a_0. The relations in Eq. (13) are weaker than those of Eq. (11) in the sense that the surface shape of the area constant simulation is not necessarily identical to the one of the volume constant simulation: stomatocyte, cup-like, and dumbbell, even branched-polymer, are allowed. We note that the surface shape of the latter simulation must be spherical

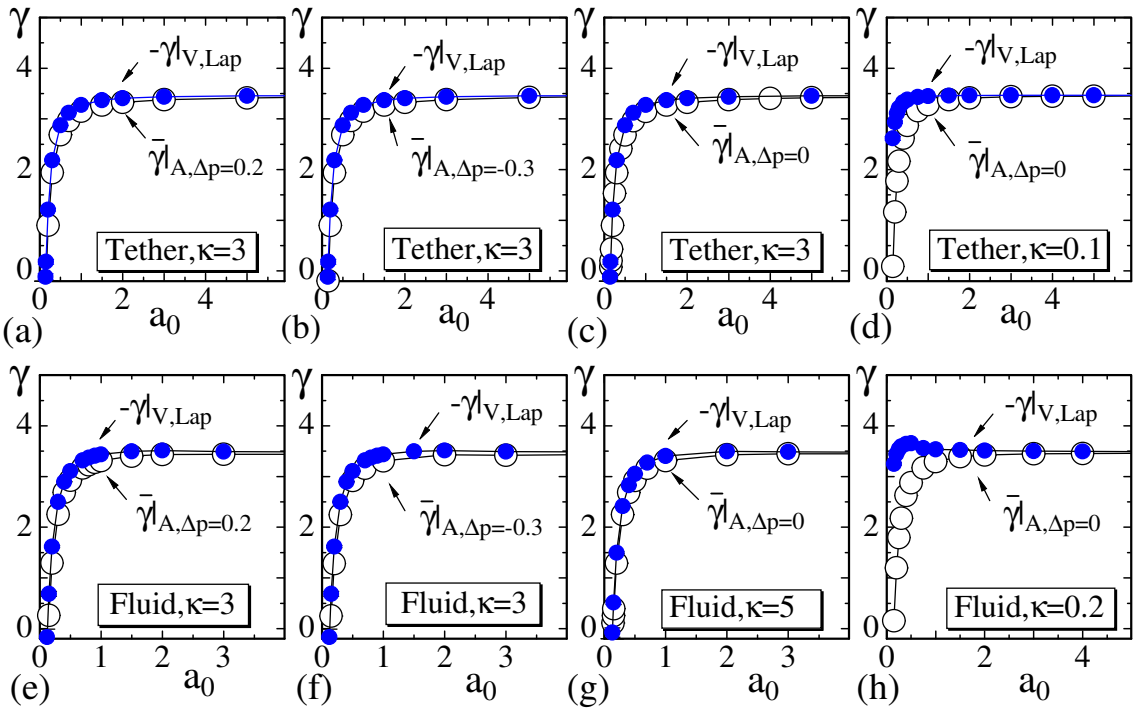

Figure 2. $-\gamma|_{V,\mathrm{Lap}}$ (•) and $\bar{\gamma}|_{A,\Delta p}$ (◯) vs. $a_0(=A_0/N_T)$ for the tethered and fluid models. $\Delta p = 0.2, -0.3, 0, 0$ are assumed for the constant area simulations. The lattice size is $N = 1442$.

because the Laplace formula for a sphere is assumed to yield $\gamma|_{V,\mathrm{Lap}}$. This requirement is always fulfilled as mentioned above.

The result that $\gamma|_{A,\Delta p=0}$ (or $-\gamma|_{V,\mathrm{Lap}}$) becomes constant in the limit of $a_0 \to \infty$ in both tethered and fluid surfaces corresponds to the experimental fact observed in biological cells [13, 14].

This work is supported in part by the Grant-in-Aid for Scientific Research (C) Number 26390138. We acknowledge the support of the Promotion of Joint Research 2014, Toyohashi University of Technology. We are grateful to K. Osari and S. Usui for the computer analyses.

References

[1] Jan Ambjörn, Bergfinnur Durhuus, and Thordur Jonsson, Phys. Rev. Lett. **58**, 2619 (1987).
[2] J. Ambjörn, A. Irbäck, J. Jurkiewicz, B. Petersson, Nucl. Phys .B**393**, Issue 3, 571 (1993).
[3] J.F. Wheater, J. Phys. A Math. Gen. **27**, 3323 (1994).
[4] W. Helfrich, Z. Naturforsch **28c**, 693 (1973).
[5] A.M. Polyakov, Nucl. Phys. B **268**, 406 (1986).
[6] D. Nelson, in Statistical Mechanics of Membranes and Surfaces, Second Edition, edited by D. Nelson, T. Piran, and S. Weinberg, (World Scientific, 2004) p.1.
[7] F. David and S. Leibler, J. Phys. II Frans **1**, 959 (1991).
[8] Jean-Baptiste Fournier and Camilla Barbetta, Phys. Rev. Lett. **100**, 078103 (2008).
[9] M. Bowick, A. Cacciuto, G. Thorleifsson, and A. Travesset, Euro. Phys. J. E **5**, 149 (2001).
[10] M. Doi and F. Edwards, *The Theory of Polymer Dynamics*, (Oxford University Press, 1986).
[11] G. Gompper and D.M. Kroll, Phys. Rev. E **51**, 514 (1995).
[12] H.Koibuchi and A.Shobukhov, Physica A **410**, 54 (2014).
[13] Ramsey A. Foty, Gabor Forgacs, Cathie M. Pfleger, and Malcolm S. Steinberg, Phys. Rev. Lett. **72**, 2298 (1994).
[14] Ramsey A. Foty, Cathie M. Pfleger, Gabor Forgacs and Malcolm S. Steinberg, Development **122**, 1611 (1996).